

# FAST ESTIMATION OF SYNCHRONIZING AND DAMPING TORQUE COEFFICIENTS USING ADALINE

Eyad. A. FEILAT

Electrical Power Engineering Department, Hijawi Faculty for Engineering Technology  
Yarmouk University, Irbid 21163, Jordan

E-mail: [eafeilat@yu.edu.jo](mailto:eafeilat@yu.edu.jo)

**Abstract:** This paper presents an adaptive technique for the estimation of the synchronizing and damping torque coefficients of a synchronous machine using a linear adaptive neuron (Adaline). The proposed technique is based on estimating the synchronizing and damping torque coefficients from online measurements of the changes of the rotor angle, rotor speed, and electromagnetic torque of the synchronous machine using Adaline architecture. These coefficients can be used as indices, which provide insight into the small-signal stability of power systems. The proposed approach can quickly predict the possible unstable conditions and hence help the operator to take the correct control action beforehand. The performance of the Adaline is compared with both Kalman filter and least-square error techniques. The Adaline offers several advantages including significant reduction in computer storage and remarkable reduction in the computational complexity, which is associated with Kalman filter. The simulation results over a wide range of operating conditions show that the Adaline can be used as efficient tool for either online or offline estimation of the synchronizing and damping torque coefficients. Therefore, it is believed that Adaline is a strong candidate for online monitoring of small-signal stability and security.

**Key words:** Small-signal stability, synchronizing and damping torque coefficients, least-square error, Kalman filter, Adaline.

## 1. Introduction

Small-signal stability analysis is concerned with the behavior of power systems under small perturbations. Its main objective is to predict the low-frequency electromechanical oscillations resulting from poorly damped rotor oscillations. The most critical types of these oscillations are the local-mode and interarea-mode oscillations [1]-[3]. The former occurs between one machine and the rest of the system, while the later occurs between interconnected machines. The study of these oscillations is very important to power system planning, operation, and control. The stability of these oscillations is a vital concern and essential for secure power system operation.

It is known that operating conditions change with time in real-time situations. These operating conditions affect the stability of the synchronous machine. Therefore, a small-signal stability analysis must be repeatedly conducted in system operation and control to provide estimates of stability indices on basis of the given data that are obtained by either measurements or computer simulation, and provide new estimates as new data are received. Traditionally, small-signal stability analysis studies of power systems are carried out in frequency domain using modal analysis method. This method implies estimation of the characteristic modes of a linearized model of the system. It requires first load flow analysis, linearization of the power system around the operating point, developing a state-space model of the power system, then computing the eigenvalues, eigenvectors, and participation factors [4].

Although eigenvalue analysis is powerful, however, it is not suitable for online application in power system operation, as it requires significantly large computational efforts. An alternative method to avoid the computational burden is to use online adaptive techniques that can quickly assess the stability of the power system on the basis of data samples obtained by measurements and automatically provides new estimates as new data samples are received.

Alternative method based on electromagnetic torque deviation has been developed. Torque deviation can be decomposed into synchronizing and damping torques [5]-[7]. The synchronizing torque is responsible for restoring the rotor angle excursion. The damping torque damps out the speed deviations. The synchronizing and damping torques are usually expressed in terms of the torque coefficients  $K_s$  and  $K_d$ . These coefficients can be calculated repeatedly and this makes it suitable for online stability assessment. In terms of  $K_s$  and  $K_d$ , both coefficients must be positive for a stable operation of the machine.

A time-domain method based on least square error (LSE) minimization technique has been applied to compute  $K_s$  and  $K_d$  for a single-machine-infinite-bus system (SMIBS) [7]. The LSE technique requires the time responses of the changes in rotor angle  $\Delta\delta(t)$ , rotor speed  $\Delta\omega(t)$ , and electromagnetic torque  $\Delta T_e(t)$ . These responses can be obtained, offline, by computer simulation or online from measured data. The significance of this method is that it permits the calculation of the torque coefficients for a machine of any degree of complexity and takes into consideration the effect of all system parameters and variables without the need for modeling assumption. This method has been extended to multimachine power systems [8], [9]. The variations of  $K_s$  and  $K_d$  over wide range of loading conditions were related to the movement of the low-frequency electrical mode. The LSE static estimation technique, however, is time consuming as it requires monitoring the entire period of oscillation.

An adaptive Kalman filter (KF) has been utilized to estimate  $K_s$  and  $K_d$  repeatedly [10]. Artificial neural network (ANN) based technique was proposed for online estimation of the synchronizing and damping torque coefficients  $K_s$  and  $K_d$  [11]. A static back propagation neural network (BPNN) has been used to associate the real and reactive power (P-Q) patterns with  $K_s$  and  $K_d$ . Although, the BPNN has very good learning ability, but it suffers from some drawbacks such as long offline training and the difficulty in determining the appropriate number of hidden layers and hidden neurons. Genetic algorithm (GA) and particle Swarm optimization (PSO) techniques have also been proposed for optimal estimation of  $K_s$  and  $K_d$  [12], [13]. Another online approach based on generalized least square (GLS) and robust fitting with bisquare weights has been proposed to estimate the synchronizing and damping torque coefficients [14]. Although the above techniques have demonstrated their effectiveness in accurate estimation of the torque coefficients, however it is believed that their computational burden makes it unsuitable for online application.

This paper presents a new technique for fast online estimation of  $K_s$  and  $K_d$  using a single adaptive linear neuron (Adaline). The technique is based on estimating  $K_s$  and  $K_d$  from the time responses of  $\Delta\delta(t)$ ,  $\Delta\omega(t)$ , and  $\Delta T_e(t)$ . Time-domain simulations are conducted over wide range of  $P$ - $Q$  loading conditions using MATLAB. The performance of the Adaline is compared with LSE and KF techniques.

## 2. Power system model

In this work, the proposed method has been tested on a system comprising a single machine connected to infinite bus power system through a transmission line. The synchronous machine is equipped with an automatic voltage regulator (AVR) and IEEE ST1A static exciter. Customarily, for small-signal stability analysis, a fourth-order model is considered for the synchronous generator. The nonlinear equations describing the dynamic behavior of a synchronous generator connected to an infinite bus through an external reactance are given in Appendix A. The system parameters are given in Appendix B. The SMIBS model is linearized at a particular operating point to obtain the linearized power system model. Figure 1 shows the well-known Phillips-Hefferon block diagram of linearized model of the SMIBS, relating the pertinent variables such as electrical torque, rotor speed, rotor angle, terminal voltage, field voltage, and flux linkages [3].

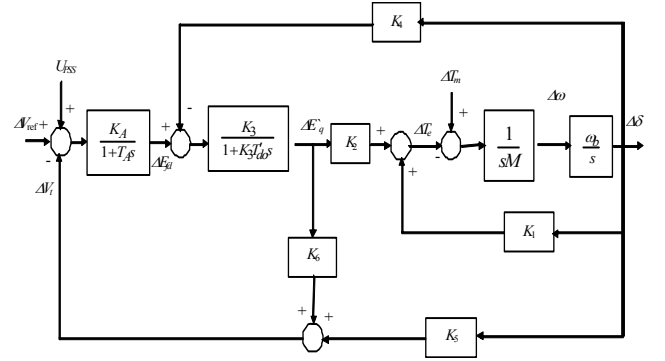


Fig. 1: Block-diagram of Phillips-Hefferon model

From the transfer function block diagram the following state-space form is developed. The system matrix  $A$  is a function of the system parameters, which depends on the operating conditions. The perturbation matrix  $B$  depends on the system parameters only. The perturbation signal  $U$  is either  $\Delta T_m$  or  $\Delta V_{ref}$ . The output matrix  $C$  relates the desired output signals vector  $Y$  to the state variables vector  $X$ , as given by (1) and (2).

The interaction among these variables is expressed in terms of the six constants  $K_1$ - $K_6$ . These constants with the exception of  $K_3$ , which is only a function of the ratio of impedance, are function of the operating real and reactive loading as well as the excitation levels in the generator. Calculations of the  $K_1$ - $K_6$  parameters and variables of the SMIBS are illustrated in Appendix C.

$$\begin{aligned}\dot{X} &= AX + BU \\ &= \begin{bmatrix} \frac{d\Delta\delta}{dt} \\ \frac{d\Delta\omega}{dt} \\ \frac{d\Delta E'_q}{dt} \\ \frac{d\Delta E_{fd}}{dt} \end{bmatrix} = \begin{bmatrix} 0 & \omega_b & 0 & 0 \\ -K_1 & -D & -K_2 & 0 \\ \frac{M}{T_{do}} & \frac{M}{T_{do}} & \frac{M}{T_{do}} & \frac{1}{T_{do}} \\ -K_A K_5 & 0 & -K_A K_6 & -1 \\ T_A & 0 & T_A & T_A \end{bmatrix} \begin{bmatrix} \Delta\delta \\ \Delta\omega \\ \Delta E'_q \\ \Delta E_{fd} \end{bmatrix} \\ &+ \begin{bmatrix} 0 & 0 \\ \frac{1}{M} & 0 \\ 0 & \frac{K_A}{K_A} \\ 0 & \frac{K_A}{K_A} \end{bmatrix} \begin{bmatrix} \Delta T_m \\ \Delta V_{ref} \end{bmatrix}\end{aligned}$$

$$Y = CX$$

$$\begin{bmatrix} \Delta\delta \\ \Delta\omega \\ \Delta T_e \end{bmatrix} = \begin{bmatrix} 1 & 0 & 0 & 0 \\ 0 & 1 & 0 & 0 \\ K_1 & 0 & K_2 & 0 \end{bmatrix} \begin{bmatrix} \Delta\delta \\ \Delta\omega \\ \Delta E'_q \\ \Delta E_{fd} \end{bmatrix} \quad (2)$$

### 3. Small-signal stability assessment using modal analysis

When a power system experiences a small disturbance as a result of small changes of loads, the system will be driven to an initial state  $X(t_0) = X_0$  at time  $t_0 = 0$ . Then, if the input is removed at  $t = t_0$ , the system respond according to the state equations

$$\dot{X} = AX \quad (3)$$

$$Y = CX$$

The state equations of the linearized model given in (3) can be used to determine the eigenvalues  $\lambda_i$  of the system matrix  $A$ , where  $\lambda_i = \sigma_i \pm j\omega_i$  are the distinct eigenvalues with a corresponding set of right and left eigenvectors  $U_i$  and  $V_i$ , respectively;  $\sigma_i$  is the damping factor and  $\omega_i$  is the damped angular frequency. The right and left eigenvectors are orthogonal, and are usually scaled to be orthonormal. The state equations of (3) can be expressed in terms of modal variables by using the modal transformation  $X = UZ$ , which leads to

$$\dot{Z} = V_i A U_i z = \Lambda Z \quad (4)$$

where  $\Lambda = \text{diag}(\lambda_i)$  [15]. Following small disturbance, the dynamic response of the system states can be described as a linear summation of various modes of oscillations

$$X(t) = \sum_{i=1}^n (V_i X_0) e^{\lambda_i t} U_i \quad (5)$$

The number of the characteristic modes  $e^{\lambda_i t}$  equals to the number of states of the linearized power system model. Real eigenvalues indicate modes, which are *aperiodic*. Complex eigenvalues indicate modes, which are oscillatory. For a complex eigenvalue  $\lambda_i = \sigma_i \pm j\omega_i$ , the amplitude of the mode varies with as  $e^{\sigma_i t}$  and frequency of the oscillation,  $f = \omega/2\pi$ . Accordingly, by expanding (5), the individual state response  $x(t)$  can be computed as

$$x(t) = \sum_{i=1}^n B_i e^{\lambda_i t} = \sum_{i=1}^n A_i e^{\sigma_i t} \cos(2\pi f_i t + \phi_i) \quad (6)$$

where  $A_i$ ,  $\sigma_i$ ,  $f_i$  and  $\phi_i$  are the  $i^{th}$  mode amplitude, damping factor, frequency, and phase angle, respectively, and  $n$  is the number of modes.

Next, a modal analysis based on the participation factors can be performed to find the specific electromechanical mode that provides the largest contribution to the low frequency oscillation [16], [17]. The participation factors provide a measure of association between the state variables and the oscillatory modes.

### 4. Small-signal stability assessment using synchronizing and damping torques

The dynamic response of a single machine connected to an infinite bus comprises various modes of oscillations. These modes of oscillations can be classified into, field and rotor circuits modes and low-frequency electromechanical modes. The oscillations of the electromagnetic torque and, consequently, the rotor oscillations are dominated by the low-frequency electromechanical modes,  $\lambda_i = \sigma_i \pm j\omega_i$ . Various methods have been proposed to break the electromagnetic torque variations into two components; the synchronizing torque component is in phase and proportional with  $\Delta\delta(t)$ , and the damping torque is in phase and proportional with  $\Delta\omega(t)$  [5]. Accordingly, the estimated torque can be written as:

$$\Delta\hat{T}_e(t) = K_s \Delta\delta(t) + K_d \Delta\omega(t) \quad (7)$$

#### 4.1 Estimation of $K_s$ and $K_d$ using LSE technique

For the reader convenience, the method of calculating the torque coefficients  $K_s$  and  $K_d$  using LSE technique is summarized. Following a small disturbance, the time responses of  $\Delta\delta(t)$ ,  $\Delta\omega(t)$ , and  $\Delta T_e(t)$ , which can be obtained from either off-line simulation or on-line measurements, are recorded as shown in Fig. 2.

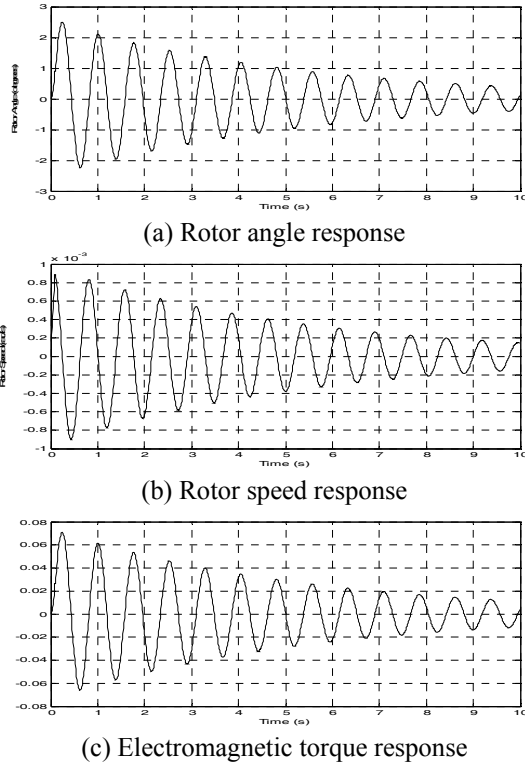


Fig. 2. Synchronous machine response.

The torque coefficients  $K_s$  and  $K_d$  are calculated using LSE by minimizing the sum of the error squared between the electric torque  $\Delta T_e(t)$  and the estimated torque  $\Delta \hat{T}_e(t)$  over the entire interval of oscillation  $T$ , where,  $T = N\Delta T$  ( $N$  is the number of samples and  $\Delta T$  is the sampling period). In matrix notation, the problem can be described by over-determined discrete system of linear equations as follows:

$$\Delta T_e(k) = AX + E(k) \quad (8)$$

$$X = A^\dagger \cdot \Delta T_e \quad (9)$$

where  $A = [\Delta\delta(k) \quad \Delta\omega(k)]$ , and  $X = [K_s \quad K_d]^T$ . Solving (9) using the left pseudo inverse of matrix  $A$  gives the values of  $K_s$  and  $K_d$  for the corresponding operating point.

#### 4.2 Estimation of $K_s$ and $K_d$ using KF technique

The Kalman filter is a recursive optimal estimator that is well suited to on-line digital processing as the data are processed recursively. It has been used extensively in estimation problems for dynamic systems. Its advantage is in its ability to handle measurements that change with time [18], [19]. Kalman filter is implemented by writing a state

equation for the parameters to be estimated in the form:

$$x_{k+1} = \phi_k x_k + w_k \quad (10)$$

$$z_k = H_k x_k + v_k \quad (11)$$

where

$x_k$  is  $n \times 1$  state vector at step  $k$ ,  $[x_1 \ x_2]^T = [K_s \ K_d]^T$ .

$\phi_k$  is  $n \times n$  state transition matrix

$v_k$  is  $n \times 1$  discrete-time random signal representing state noise

$z_k$  is  $m \times 1$  measurement vector at step  $k$

$H_k$  is  $m \times n$  measurement matrix

$w_k$  is  $n \times 1$  discrete-time random signal representing measurement errors.

Equations (10) and (11) represent the state equation of the parameters to be estimated in time, and the measurements which refer to the samples of the electromagnetic torque at step  $k$ , respectively. The measurement equation of the electromagnetic torque can be written as:

$$\Delta T_{e_k} = [\Delta\delta_k \quad \Delta\omega_k] \begin{bmatrix} x_1 \\ x_2 \end{bmatrix} + v_k \quad (12)$$

#### 4.3 Estimation of $K_s$ and $K_d$ using Adaline

The Adaline is introduced in [20] as a powerful harmonics tracking technique. It produces a linear combination of its input vector  $X(k) = [x_1, x_2, \dots, x_n]$  at time  $k$ . After, the input vector is multiplied by the weight vector  $W(k) = [w_1, w_2, \dots, w_n]$ , the weight inputs are combined to produce the linear output  $\hat{y}(k) = W(k)^T \cdot X(k)$ . The weight vector is adjusted by an adaptation rule so that the output from the Adaline algorithm  $\hat{y}(k)$  is close to the desired value  $y(k)$ . The least mean square (LMS) algorithm, known as the modified Widrow-Hoff delta rule, is usually used as the adaptation rule. This rule is given by:

$$W(k+1) = W(k) + \frac{\alpha e(k) X(k)}{\lambda + X(k)^T X(k)} \quad (13)$$

where  $e(k) = y(k) - \hat{y}(k)$  is the prediction error at time  $k$ ,  $\hat{y}(k)$  is the estimated signal magnitude, and  $\alpha$  is the learning parameter (reduction factor), and  $\lambda$  is a parameter to be suitably chosen to avoid division by zero. Perfect training is attained when the error is brought to zero. The numerical values of  $\alpha$  and  $\lambda$  greatly affects the performance of the estimation, which is demonstrated in the simulation.

Alternatively, a modified Widrow-Hoff delta rule is used to produce fast convergence for estimating  $K_s$  and  $K_d$ . The Adaline weight vector is adapted as

$$W(k+1) = W(k) + \frac{\alpha e(k) \text{sgn}(X(k))}{\lambda + X(k)^T \text{sgn}(X(k))} \quad (14)$$

where the sgn function is given by

$$\text{sgn}(x_i) = \begin{cases} +1 & \text{if } x_i > 0 \\ -1 & \text{if } x_i < 0 \end{cases} \quad (15)$$

The Adaline algorithm is characterized by simple calculations, which lead to a fast execution processing time of the algorithm, a property, which is essential for online application [21].

## 5. Adaline training

The Adaline algorithm is utilized in this study to approximate the torque deviation  $\Delta \hat{T}_e(k)$  as a linear combination of the synchronizing torque  $K_s \Delta \delta(k)$  and the damping torque  $K_d \Delta \omega(k)$ :

$$\Delta \hat{T}_e(k) = [w_1(k) \quad w_2(k)] \begin{bmatrix} \Delta \delta(k) \\ \Delta \omega(k) \end{bmatrix} \quad (16)$$

Figure 3 shows the Adaline block diagram based estimator of  $K_s$  and  $K_d$ , where  $\Delta \delta(k)$  and  $\Delta \omega(k)$  are given as inputs to the single neuron,  $\Delta \hat{T}_e(k)$  is the output of the Adaline,  $\Delta T_e(k)$  is desired output torque and  $w_1(k)=K_s$  and  $w_2(k)=K_d$  [21].

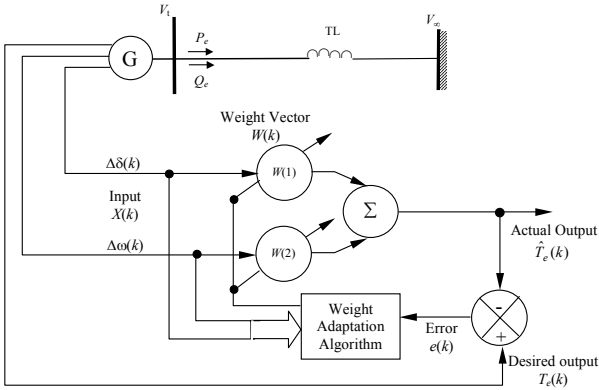


Fig. 3. A schematic diagram of Adaline-based estimator of  $K_s$  and  $K_d$  of a SMIBS.

## 6. Simulation results

This paper is an extension of the work presented in [21]. Performance evaluation of both Adaline schemes, for the estimation of  $K_s$  and  $K_d$ , is compared with LSE and KF estimation techniques. The evaluation is carried out by conducting several offline simulation cases on the linearized model of the SMIBS. Either the state-space model or the Phillips-Hefferon block diagram implemented in SIMULINK can be used for offline simulation. The system input is a 0.1 pu mechanical torque pulse

( $\Delta T_m$ ) for 10 ms. The system output vector comprises the rotor speed, rotor angle, and electromagnetic torque. A sampling rate of 100 samples per second, over a window size of 10 seconds, is set for all simulation cases. Starting with zero initial weights  $W(k)$ , the rotor angle  $\Delta \delta(k)$  and rotor speed  $\Delta \omega(k)$  are fed to the Adaline as input signals, whereas the developed torque  $\Delta T_e(k)$  is introduced to the Adaline as the desired signal. The output of the Adaline is given as  $\Delta \hat{T}_e(k) = w_1(k) \Delta \delta(k) + w_2(k) \Delta \omega(k)$ .

Figures 4-5 and Figures 6-7 show the results of Adaline estimation using equations (13) and (14), respectively, for stable and unstable operating conditions. The Adaline performance is compared with KF and LSE estimation. It can be seen that Kalman filter gives faster convergence and rigid tracking, in particular for  $K_s$ , without overshoot. However, the accurate estimation of  $K_s$  and  $K_d$  and the light computational burden of the Adaline algorithms make its implementation easier than KF. It is crucial to tune the parameters  $\alpha$  and  $\lambda$  for the Adaline using trial and error to achieve a high online tracking accuracy of  $K_s$  and  $K_d$ . The final estimates of  $K_s$  and  $K_d$  for stable and unstable operating points are given in Table 1.

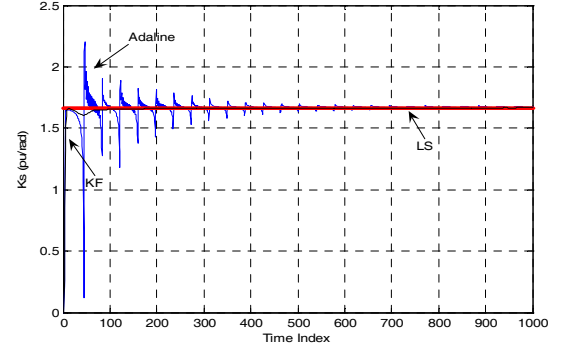


Fig. 4-a

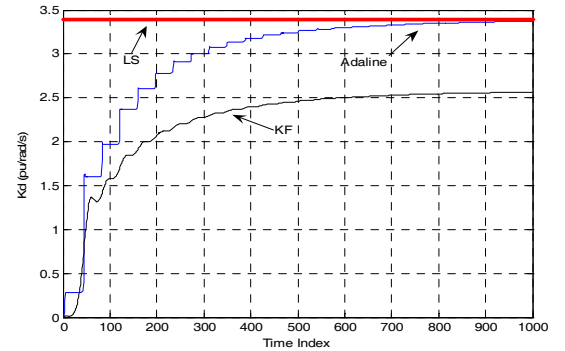


Fig. 4-b

Fig. 4. Adaline-1 and KF estimation of  $K_s$  and  $K_d$ .  $V_{to}=1.05$  pu;  $P_e=0.8$  pu;  $Q_e=-0.6$  pu.

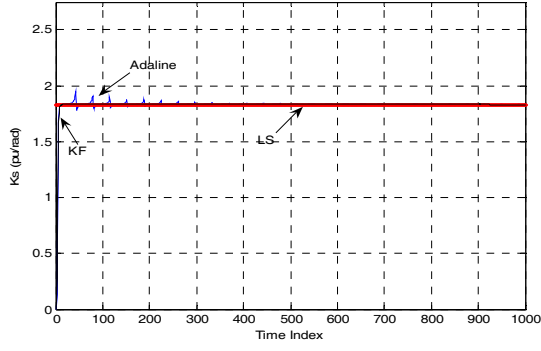


Fig. 5-a

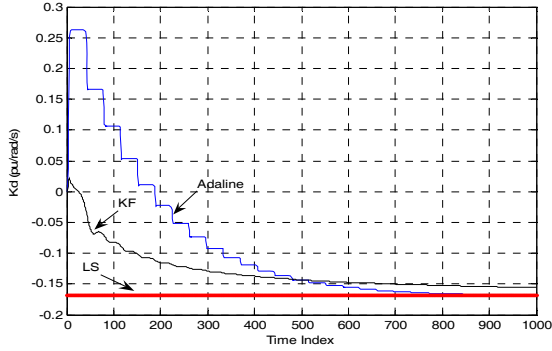


Fig. 5-b

Fig. 5. Adaline-1 and KF estimation of  $K_s$  and  $K_d$ .  $V_{to}=1.05$  pu;  $P_e=0.8$  pu;  $Q_e=0.60$  pu.

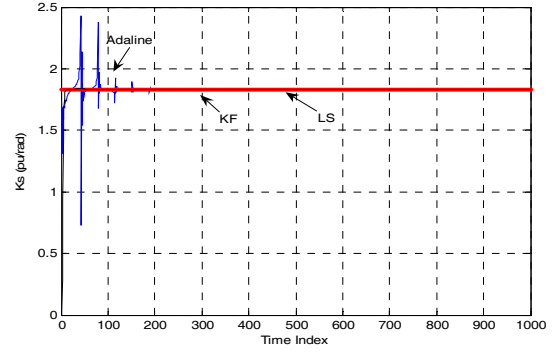


Fig. 7-a

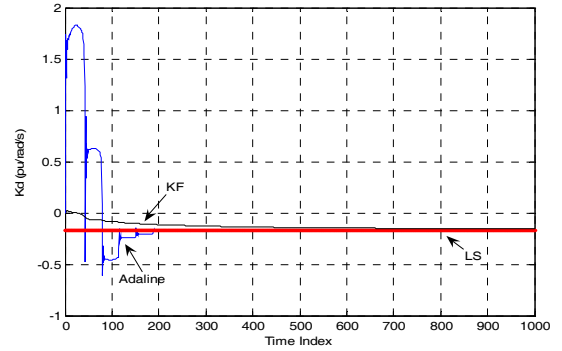


Fig. 7-b

Fig. 7. Adaline-2 and KF estimation of  $K_s$  and  $K_d$ .  $V_{to}=1.05$  pu;  $P_e=0.8$  pu;  $Q_e=0.60$  pu.

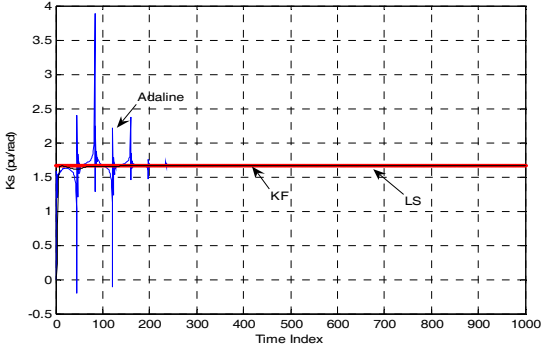


Fig. 6-a

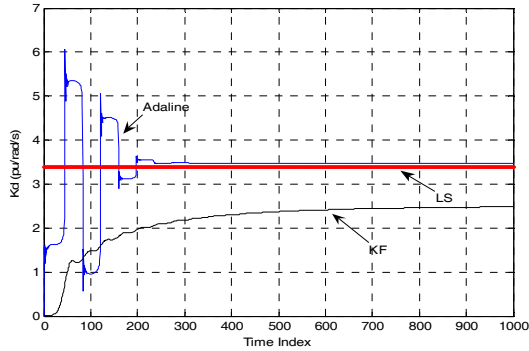


Fig. 6-b

Fig. 6. Adaline-2 and KF estimation of  $K_s$  and  $K_d$ .  $V_{to}=1.05$  pu;  $P_e=0.8$  pu;  $Q_e=-0.6$  pu.

As can be seen in Table 1 both Adaline schemes give more accurate estimation of  $K_d$  in comparison with KF estimation. The estimation of  $K_s$  and  $K_d$  over a wide range of operating conditions using Adaline-1 is shown in Fig. 8. It is observed from Fig. 8 that  $K_s$  and  $K_d$  varies with the  $P_e$  and  $Q_e$  which characterize the generator loading conditions. In the estimation process of  $K_s$  and  $K_d$  indices, the values of  $\alpha$  and  $\lambda$  are fixed at  $\alpha=1.98$  and  $\lambda=0.0001$ . Therefore, the proposed Adaline can be employed to yield the estimates of  $K_s$  and  $K_d$  for any monitored loading condition ( $P_e$  and  $Q_e$ ) at any terminal voltage  $V_t$  in real-time based on measurements of rotor angle, rotor speed, and electromagnetic torque time responses.

Table 1: Final estimates of  $K_s$  and  $K_d$

Rotor Mode	Estimates of Torque Coefficients				
	$K_i$	LSE	KF	Adaline1 $\alpha=1.98$	Adaline2 $\alpha=1.50$
-0.188 $\pm j8.257$ stable	$K_s$	1.667	1.667	1.679	1.675
	$K_d$	3.389	2.566	3.375	3.478
0.009 $\pm j8.635$ unstable	$K_s$	1.832	1.832	1.832	1.832
	$K_d$	-0.168	-0.156	-0.169	-0.169

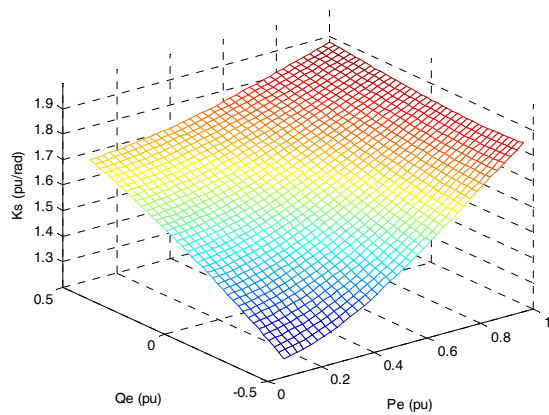


Fig. 8-a

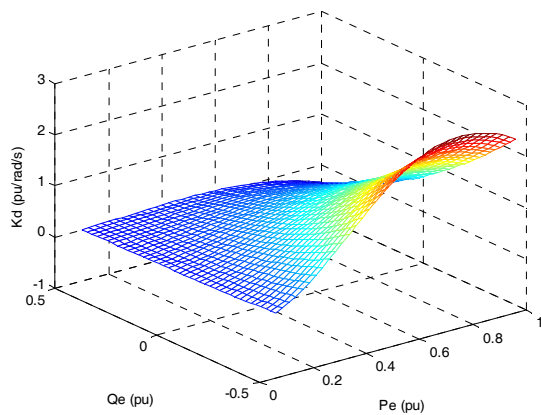


Fig. 8-b

Fig. 8. Estimated value of  $K_s$  and  $K_d$  over a wide range of operating condition ( $P_e$  and  $Q_e$ )

## 7. Conclusion

An online adaptive technique for accurate estimation of the synchronizing and damping torque coefficients,  $K_s$  and  $K_d$ , using Adaline is presented in this paper. The performance of the technique has been compared with KF and LSE techniques. Simulation results have shown that Adaline technique is accurate and can be implemented with small computing time and storage. It is believed, that Adaline is a good candidate for online estimation of small signal stability indices.

## References

1. Rogers, G.: *Power System Oscillations*. Kluwer Academic Publisher, 2000.
2. Kundur, P.: *Power System Stability and Control*, McGraw-Hill, 1994.
3. Yu, Y. N.: *Electric Power System Dynamics*, Academic Press, 1983.
4. Hsu Y.Y., Chen, C.L.: *Identification of Optimum Location for Stabilizer Applications using Participation Factors*. In: IEE Proc. Gen., Trans. & Distr., Pt. C, Vol. 134, No.3, 1987, p. 238-244.
5. Demello F.P., Concordia, C.: *Concepts of synchronous stability as affected by excitation control*. In: IEEE Trans. Power Apparatus and Systems, Vol.PAS-88, No.4, April 1969, p.316-329.
6. deOliveria, S.E.M.: *Synchronizing and Damping Torque Coefficients and Power System Steady-State Stability as Affected by Static VAR Compensation*. In: IEEE Trans. Power Systems, Vol.PWRS-9, No.1, February 1994, p. 109-119.
7. Alden, R.T.H., Shaltout, A.A.: *Analysis of damping and synchronizing torques: Part-I: A general calculation method*. In: IEEE Trans. Power Apparatus and Systems, Vol.PAS-98, No.5, September/October 1979, p. 1696-1700.
8. Shaltout, A., Feilat, E.A.: *Damping and synchronizing torque computation in multimachine power systems*. In: IEEE Trans. on Power Systems, Vol.PWRS-7, No.1, February 1992, p. 280-286.
9. Shaltout, A., Feilat, E.A.: *Damping and synchronizing torque of closely coupled generators*. In: Electric Power System Research, Vol. 26, No.2, 1993, p. 195-202.
10. Feilat, E.A., Younan, N., Grzybowski, S.: *Estimating the synchronizing and damping torque coefficients using Kalman filtering*. In: Electric Power Systems Research, Vol.52, No.2, 1999, p. 145-149.
11. Feilat, E.A., Aggoune, E.M., Bettayeb, M., Al-Duwaish, H.: *On-line estimation of synchronizing and damping torque coefficients using neural network based approach*. In: Electric Machines and Power Systems, Vol.25, 1997, p. 993-1007.
12. EL-Naggar, K.M., AL-Othman, A.: *Genetic based algorithms for estimating synchronizing and damping torque coefficients*. In: Proceedings of Fourth IASTED International Conference on Power and Energy Systems (EuroPES 2004), Rhodes, Greece, 2004, p. 356-360.
13. AL-Othman, A.K., EL-Naggar, K.M.: *Estimating synchronizing and damping torque coefficients using particle Swarm optimization*. In: Proceedings of the Fifth IASTED International Conference on Power and Energy Systems (EuroPES 2005), Benalmádena, Spain, June 15-17, 2005.
14. Ghasemi, H., Cañizares, C.: *Damping torque estimation and oscillatory stability margin prediction*. In: Proceedings of IEEE PES Summer Meeting, Montreal, Canada, June 2006.
15. Kailth, T.: *Linear Systems*, Prentice-Hall, NJ, 1980.
16. Hiroshi Suzuki, Soichi Takeda, Yoshizo Obata: *An efficient eigenvalue estimation technique for multimachine power system dynamic stability analysis*. In: Electric Engineering in Japan, Vol.100, No.5, 2007, pp. 45-53.

17. Lucas, J.R., Annakkage, U.D., Karawita, C., Muthumuni, D., Jayasinghe, R.P.: *Inclusion of small signal stability assessment to electromagnetic transient programs*. In: Proceedings of Power and Energy System Conference, April 2-4, 2008, Langkawi, Malaysia.
18. Girgis, A.A., Daniel Hwang, T.L.: *Optimal estimation of voltage phasors and frequency deviation using linear and non-linear Kalman filtering: theory and limitations*. In: IEEE Trans. Power Apparatus and Systems, Vol.PAS-103, No.10, October 1984, p. 2943-2949.
19. Girgis, A.A., Makram, E.: *Application of Adaptive Kalman Filtering in Fault Classification, Distance Protection, and Fault Location Using Microprocessors*. In: IEEE Trans. Power Systems, Vol.3, No.1, February 1988, p. 301-309.
20. Dash, P.K., Swain, D.P., Liew, A.C., Saifur Rahman, . *An adaptive linear combiner for on-line tracking of power system harmonics*. In: IEEE Trans. Power Systems, Vol.PWRS-11, No.4, November 1996, p. 1730-1735.
21. Feilat, E.A.: *Fast Estimation of synchronizing and damping torque coefficients using an adaptive neural network*. In: Proceedings of 42<sup>nd</sup> International Universities Power Engineering Conference (UPEC 2007), 4-6 September, 2007, University of Brighton, Suusex, UK.

## Appendix A

The dynamical nonlinear differential equations of the SMIBS are given below [4]:

$$\frac{d\omega}{dt} = \frac{1}{M}(T_m - T_e) \quad (A-1)$$

$$\frac{d\delta}{dt} = \omega_b(\omega - 1) \quad (A-2)$$

$$\frac{dE'_q}{dt} = \frac{1}{T'_{do}} [E_{fd} - E'_q - (x_d - x'_d)i_d] \quad (A-3)$$

$$\frac{dE_{fd}}{dt} = \frac{1}{T_A} [K_A(V_{ref} - v_t + u_{PSS}) - E_{fd}] \quad (A-4)$$

where  $T_m$  and  $T_e$  are the mechanical input and electrical output torques of the generator, respectively;  $M$  is inertia constant.  $E_{fd}$  is the field voltage;  $T_{do}$  is the open circuit field time constant;  $x_d$  and  $x'_d$  are the  $d$ -axis and transient reactances of the generator, respectively.  $K_A$  and  $T_A$  are the gain and time constant of the excitation system, respectively.  $V_{ref}$  is the reference voltage.

## Appendix B

The parameters of the synchronous generator and transmission line are given below [4].

*Machine Parameters (pu)*

$$x_d = 0.973, x_q = 0.550, x'_d = 0.190$$

$$M = 9.26, T_{do} = 7.76 \text{ s}, D = 0, \omega_b = 377 \text{ rad/s}$$

*Exciter:*

$$K_A = 50, T_A = 0.05 \text{ s}$$

*Transmission Line (pu)*

$$r_e = 0.0, x_e = 0.40$$

*Nominal Operating Point (pu)*

$$P_{eo} = 0.9, Q_{eo} = 0.1, V_{to} = 1.05$$

## Appendix C

For a SMIBS the following relationships apply with all the variables with subscript o are calculated at their pre-disturbance operating values corresponding to the operating conditions  $P_o, Q_o$ , and  $V_{to}$ . [5]:

$$i_{qo} = \frac{P_o V_{to}}{\sqrt{(P_o x_q)^2 + (V_{to}^2 + Q_o x_q)^2}} \quad (C-1)$$

$$v_{do} = i_{qo} x_q \quad (C-2)$$

$$v_{qo} = \sqrt{V_{to}^2 - v_{do}^2} \quad (C-3)$$

$$i_{do} = \frac{Q_o + x_q i_{qo}^2}{v_{qo}} \quad (C-4)$$

$$E_{qo} = v_{qo} + i_{do} x_q \quad (C-5)$$

$$E_o = \sqrt{(v_{do} + x_e i_{qo})^2 + (v_{qo} - x_e i_{do})^2} \quad (C-6)$$

$$\delta_o = \tan^{-1} \left( \frac{v_{do} + x_e i_{qo}}{v_{qo} - x_e i_{do}} \right) \quad (C-7)$$

For the case  $r_e = 0$ ,  $K_1$ - $K_6$  constants are calculated as:

$$K_1 = \frac{x_q - x'_d}{x_e + x'_d} i_{qo} E_o \sin \delta_o + \frac{1}{x_e + x_q} E_{qo} E_o \cos \delta_o \quad (C-8)$$

$$K_2 = \frac{E_o \sin \delta_o}{x_e + x'_d} \quad (C-9)$$

$$K_3 = \frac{x_e + x'_d}{x_e + x_d} \quad (C-10)$$

$$K_4 = \frac{x_d - x'_d}{x_e + x'_d} E_o \sin \delta_o \quad (C-11)$$

$$K_5 = \frac{x_q}{x_e + x_q} \frac{v_{do}}{V_{to}} E_o \cos \delta_o - \frac{x'_d}{x_e + x'_d} \frac{v_{qo}}{V_{to}} E_o \sin \delta_o \quad (C-12)$$

$$K_6 = \frac{x_e}{x_e + x'_d} \frac{v_{qo}}{V_{to}} \quad (C-13)$$